Biogeosciences Discuss., 10, 1957–1992, 2013
www.biogeosciences-discuss.net/10/1957/2013/
doi:10.5194/bgd-10-1957-2013

Biogeosciences Discussions Open Access

Detecting tropical forest biomass dynamics from repeated airborne Lidar measurements

V. Meyer[1], S. S. Saatchi[1], J. Chave[2], J. Dalling[3], S. Bohlman[4], G. A. Fricker[5], C. Robinson[5], and M. Neumann[1]

[1]Jet Propulsion Laboratory, California Institute of Technology, 4800 Oak Grove Drive, Pasadena, CA 91109, USA
[2]CNRS, Laboratoire Evolution et Diversité Biologique, UMR5174, Université Paul Sabatier, 31062 Toulouse cedex, France
[3]Department of Plant Biology, University of Illinois, Urbana, IL 61801, USA
[4]School of Forest Resources and Conservation, University of Florida, Gainesville, FL 32611, USA
[5]Department of Geography, University of California, 1255 Bunche Hall Box 951524, Los Angeles, CA 90095, USA

Received: 16 January 2013 – Accepted: 19 January 2013 – Published: 5 February 2013

Correspondence to: V. Meyer (victoria.meyer@jpl.nasa.gov)

Published by Copernicus Publications on behalf of the European Geosciences Union.

Abstract

Reducing uncertainty of terrestrial carbon cycle depends strongly on the accurate estimation of changes of global forest carbon stock. However, this is a challenging problem from either ground surveys or remote sensing techniques in tropical forests. Here, we examine the feasibility of estimating changes of tropical forest biomass from two airborne Lidar measurements acquired about 10 yr apart over Barro Colorado Island (BCI), Panama from high and medium resolution airborne sensors. The estimation is calibrated with the forest inventory data over 50 ha that was surveyed every 5 yr during the study period. We estimated the aboveground forest biomass and its uncertainty for each time period at different spatial scales (0.04, 0.25, 1.0 ha) and developed a linear regression model between four Lidar height metrics and the aboveground biomass. The uncertainty associated with estimating biomass changes from both ground and Lidar data was quantified by propagating measurement and prediction errors across spatial scales. Errors associated with both the mean biomass stock and mean biomass change declined with increasing spatial scales. Biomass changes derived from Lidar and ground estimates were largely (36 out 50 plots) in the same direction at the spatial scale of 1 ha. Lidar estimation of biomass was accurate at the 1 ha scale (R^2 = 0.7 and $RMSE_{mean}$ = 28.6 Mg ha^{-1}). However, to predict biomass changes, errors became comparable to ground estimates only at about 10-ha or more. Our results indicate that the 50-ha BCI plot lost a significant amount of biomass (-0.8 ± 2.2 Mg ha^{-1} yr^{-1}) over the past decade (2000–2010). Over the entire island and during the same period, mean AGB change is -0.4 ± 3.7 Mg ha^{-1} yr^{-1}. Old growth forests lost biomass (-0.7 ± 3.5 Mg ha^{-1} yr^{-1}), whereas the secondary forests gained biomass ($+0.4 \pm 3.4$ Mg ha^{-1} yr^{-1}). Our analysis demonstrates that repeated Lidar surveys, even with two different sensors, is able to estimate biomass changes in old-growth tropical forests at landscape scales (>10 ha).

1 Introduction

Tropical forests are a major focus for research because of the role they play in the global carbon cycle and recently in climate mitigation policies through REDD protocols (Reduced Emissions from Deforestation and Degradation). The study of forest dynamics is of particular interest because changes in carbon fluxes over time are caused by either natural or anthropogenic disturbances and by recovery from these disturbances. The study of carbon flux measurements in tropical forests has shown unprecedented progress in recent years, based on both ground and remote sensing techniques. For ground-based data, allometric equations have been developed from tree inventory data made across a range of tropical forest types (Chave et al., 2005; Higuchi et al., 1994; Chambers et al., 2001). These equations are key to converting tree diameter, height, and wood specific density into tree aboveground biomass (AGB, measured in oven-dry mass units) and to infer stand AGB across spatial scales (Chave et al., 2004). However, forest structure and biomass distribution are spatially variable and ground sampling and monitoring of tropical forest carbon dynamics is fraught with large uncertainties (Clark and Clark, 2000; Saatchi et al., 2011).

Remote sensing approaches, particularly from Lidar or low frequency radar sensors have been shown to provide relatively accurate estimates of above ground biomass over large areas (Asner et al., 2010; Drake et al., 2002a; Lefsky et al., 2002; Saatchi et al., 2011). High resolution Lidar data from airborne platforms have proven to be the most commercially available, cost effective, and accurate means of assessing forest above ground carbon stock for policy driven projects (Asner et al., 2011). Lidar measurements provide three dimensional forest structure at high enough spatial resolution to capture several important measures of forest dynamics: (1) tree size structure representing successional stages of the forest (Ni-Meister, et al., 2001), (2) gap size and light conditions in the forest capturing the disturbance dynamics and conditions for forest carbon dynamics (Lefsky et al., 2002; Kellner and Asner, 2009), and (3) spatial

patterns representing changes of forest structure and biomass from tree to landscape scales (Dubayah et al., 2010).

The recent literature on this topic has mostly focused on measuring tropical forest carbon stocks. Comparatively limited research has been devoted to assessing the capability of remote sensing data to detect changes of forest biomass (but see Dubayah et al., 2010). The vertical height profiles can be used to develop algorithms for biomass change detection at various spatial scales using high resolution small footprint lidar or medium footprint waveform Lidar sensors (Dubayah et al., 2010). In this paper, we test this approach over the period 1998–2009 in the tropical forest of Barro Colorado Island (BCI), Panama. We seek to quantify the uncertainty for both AGB stocks and change at three different spatial scales (1 ha, 0.25 ha and 0.04 ha) using two different Lidar sensors. We then quantify the errors at different spatial scales and extend the analysis of local scale carbon dynamics in the 50 ha plot to the entire Barro Colorado Island. The analysis allows us to examine at what scale, we are able to detect the spatial patterns of forest biomass change while providing stable and accurate estimates.

2 Material and methods

2.1 Study area and inventory data

Barro Colorado Island (BCI) is a 1500 ha island located in the Panama Canal Zone in Central Panama. It was isolated from the mainland after the Chagres River was dammed in 1910 to complete the Panama Canal (McCullough, 1977, Fig. 1). The island is administered by the Smithsonian Tropical Research Institute (STRI) as part of the Barro Colorado Nature Monument (BCNM), a protected national biological reserve since 1923. Detailed description of climate, flora and fauna of BCI can be found in Croat (1978) and Leigh (1999). BCI is covered by moist tropical forest with half of the island dominated by old secondary forests (approximately 100 yr old), for the most part growing back from agricultural clearings, while the rest is covered by forests that

were left relatively undisturbed over the past 200–400 yr except for some selective logging (Kenoyer, 1929; Foster, 1982). Forest canopy can attain 35–40 m, although some emergent trees reaching 50 m are mentioned in the literature (Leigh and Wright, 1990; Leigh et al., 2004). The island receives an average of 2600 mm of rainfall per year. A four months dry season usually begins in January and ends in April, when 12 % of the canopy species (maximum height > 10 m) lose their leaves (Leigh and Wright, 1990; Condit et al., 2000).

In this study, we used the BCI 50 ha forest dynamics plot managed by the Center for Tropical Forest Science (CTFS). The plot is located in an area with low elevational variation in the center of the island (Condit, 1995). The inventory data was first collected in 1982, then every five years since 1985, with the most recent census in 2010. We use the census data collected during the 2000, 2005 and 2010 to match the ground measurements with the remote sensing data. Each census included all trees with diameter at breast height (DBH) greater than 1 cm, with measurements made higher on the bole, for individuals with buttresses or trunk irregularities. All trees in the census are tagged, measured, mapped and identified to species.

Tree AGB was obtained from allometric equations in Chave et al. (2005). The AGB estimate is derived from tree DBH, height and wood density. Height was inferred from DBH using species-specific equations (Supplement). Here, we only included the trees with DBH > 10 cm for AGB estimation, which represent about 10 % of all trees in the plot (Supplement).

We divided the 50 ha plot into three spatial scale subplots of 0.04 ha (20 m × 20 m), 0.25 ha (50 m × 50 m) and 1 ha (100 m × 100 m) to compute forest biomass and biomass change. Each subplot was identified by the coordinates of its four corners and was co-located on the remote sensing data for further analysis.

2.2 Ground estimates of biomass change

The AGB estimates for a three census period including the most recent one in 2010 were used to quantify biomass change within the 50 ha plot at the three spatial scales

mentioned above. We calculated the mean and standard deviation of AGB estimates by propagating errors due to DBH measurement and to the allometric model (see Supplement). Ground-estimated AGB was then used to determine AGB change in the 50 ha plot between 2000 and 2010, using the plot census data from 2000, 2005 and 2010. This analysis was also performed at three spatial scales using the mean AGB density and other statistics in order to quantify the changes of biomass density through time and the uncertainty associated with estimating changes from census data.

2.3 Airborne Lidar data

Our study uses airborne Lidar data acquired by two different sensors over BCI approximately 10 yr apart. Both sensors scanned the landscape to measure the surface elevation and the vegetation vertical structure. We used the Laser Vegetation Imaging Sensor (LVIS) medium footprint Lidar dataset acquired in March 1998 (20 m footprint) and a small footprint discrete return Lidar (DRL) dataset acquired in August and September 2009 (1 m footprint) (Supplement). Relative height (RH) quartiles RH25, RH50, RH75 and RH100 were produced for both LVIS and DRL data (Supplement) at 0.04, 0.25, and 1.0 ha resolution over the entire island. The metrics respectively represent the 25 %, 50 %, 75 %, and 100 % percentile of energy from the Lidar waveforms developed at each scale of analysis and represent vegetation in the four quartiles of height in the forest. These metrics are useful predictors of biomass and canopy vertical structure in forest (Drake et al., 2002a,b, 2003; Duong et al., 2008). We performed a cross-calibration between the two data sets using a filter to improve the LVIS ground elevation estimation (Fricker et al., 2012) (Supplement). After calibration, LVIS's height metrics were adjusted to allow comparisons between the two datasets and to detect changes of forest structure and biomass over the landscape and at different spatial scales. The DRL data did not need any further calibration.

2.4 AGB estimation from Lidar

We used the field-estimated AGB for the 2000 and 2010 censuses to calibrate the 1998 LVIS and 2009 DRL data, respectively. During the calibration, we did not attempt to adjust the ground biomass data to match the year of Lidar flights as such a process would be subject to errors due to uncertainty in forest growth and disturbance rates. The calibration was performed at the three aforementioned scales using linear regression models between AGB and LVIS and DRL height metrics (Supplement).

We developed models between Lidar metrics and AGB at each scale. The models were created using one value of each RH metric (RH25, RH50, RH75 and RH100) per subplot. A multiple regression model was created for each sensor at each of the three scales, using the coefficients calculated with the models.

$$\mathrm{AGB}_{\mathrm{LVIS}} = (a_0 + a_1\mathrm{RH25} + a_2\mathrm{RH50} + a_3\mathrm{RH75} + a_4\mathrm{RH100} + a_5\mathrm{RH100}_{\mathrm{max}})^2 \quad (1)$$

$$\mathrm{AGB}_{\mathrm{DRL}} = (a_0 + a_1\mathrm{RH25} + a_2\mathrm{RH50} + a_3\mathrm{RH75} + a_4\mathrm{RH100})^2 \quad (2)$$

where the coefficients inferred from the fitting procedure are provided in Table 1. We used a stepwise multiple regression model and relative importance analysis to evaluate the importance of each variable in explaining the variability of biomass at different scales. The analysis is performed in the R statistical computing environment. The stepwise analysis uses the Akaike's information criteria (AIC) to select models and maximize the likelihood of the response by minimizing the number of parameters. The relative importance analysis was performed to quantify the portion of the coefficient of determination (R^2) attributable to the parameter (as predictor) when the parameters are correlated in the regression analysis (Chao et al., 2012). A "leave-20 %-out" cross-validation was performed to assess the predictive performance of our models with both Lidar sensors. This cross-validation uses 20 % of the original data as the validation data, while the remaining 80 % are used as the training data. This operation is repeated until all the observations are used as the validation data once. This method is similar to the K-fold cross-validation method, where $K = 5$. The 1 ha scale AGB results

were then aggregated to get numbers at larger scales (5 ha, 10 ha and 25 ha). Due to lack of points at larger scales for performing the statistical analysis, we only report the comparison of aggregated numbers with the field observations.

Equations (1) and (2) derived from the 1ha scale analysis were then applied on Lidar data acquired over the entire Barro Colorado Island to predict the spatial distribution of biomass outside the BCI 50 ha plot. We extended the analysis by calculating the AGB change over the entire island from the two maps generated from each Lidar sensor. To relate the changes of the forest AGB to landscape features, the change map was further analyzed by classifying the forests of the island into two age groups, based on an available forest age map (Mascaro et al., 2011a; from Enders, 1935). The age groups included areas of forest older than 400 yr, hereafter called "old growth forest", and areas of forest younger than 130 yr, classified as "secondary forest." Using the age map, we analyzed the magnitude and spatial patterns of the forest biomass change over the island.

3 Results

3.1 Field estimates of forest biomass dynamics

The analysis of the spatial structure of the forest within the 50 ha permanent plot shows that 1 ha subplots give stable estimates of AGB with low spatial variance, while at 0.04 ha subplots estimates of AGB have high spatial variability dominated by the spatial variability of large trees. In 2010, AGB ranged between 21 and 1838 Mg ha^{-1} in 0.04 ha subplots (coefficient of variation = 0.75), showing high AGB variation, as compared with 116 to 369 Mg ha^{-1} in 1 ha subplots (coefficient of variation = 0.18) (Table 2). The AGB distribution shown in Fig. 2a is clearly skewed towards low biomass values when working with small subplots of 0.04 ha (skewness = 3.05) but is more symmetrical when using 1 ha subplots (skewness = 0.45). The presence or absence of a single

large tree in a 0.04-ha subplot will strongly impact the AGB value of a subplot, leading to extremely low or extremely high AGB values (Chave et al., 2003).

AGB, estimated at the 1 ha scale, decreased both between 2000 and 2005 and between 2005 and 2010 census periods in the 50 ha plot (Fig. 2b, Table 3). The histograms show that changes between 2000 and 2005 were slightly skewed to negative values and had only few extreme values (mean = $-2.4\,Mg\,ha^{-1}$, std = $10.5\,Mg\,ha^{-1}$), whereas during the second period between 2005 and 2010, there were more extreme values and the biomass loss was larger (mean = $-5.5\,Mg\,ha^{-1}$, std = $16.1\,Mg\,ha^{-1}$). AGB in the 50 ha plot dropped by $7.8\,Mg\,ha^{-1}$ (std = $17.6\,Mg\,ha^{-1}$) over the 10-yr period of study (i.e. an average value of $0.8\,Mg\,ha^{-1}\,yr^{-1}$).

The spatial scale analysis of AGB change (Table 3) confirms that at the 1 ha scale, the observed changes are more stable for a long-term analysis than smaller subplots ($std_{change2000/2010\_1\,ha} = 17.6\,Mg\,ha^{-1}$ and $std_{change2000/2010\_0.04\,ha} = 107.4\,Mg\,ha^{-1}$). Here, stability refers to less variability and suggests that larger plots are individually more reliable for detecting long-term changes, whereas smaller plots individually represent changes associated with both natural gap dynamics (disturbance and recovery) and long term changes. Furthermore, 37 1 ha subplots lost AGB and the rest gained AGB over the same period. By further aggregating the subplots to larger scales, we find the forest is losing biomass more uniformly at 5-ha scale (std = $5.9\,Mg\,ha^{-1}$), and at 10-ha scale (std = $4.2\,Mg\,ha^{-1}$). At 25 ha, the two subplots lost -7.7 and $-8.0\,Mg\,ha^{-1}$ of AGB for an average value of $-7.8\,Mg\,ha^{-1}$ at 50 ha between 2000 and 2010.

3.2 Lidar-derived biomass estimation

Although the relative height (RH) metrics were individually correlated with ground-based AGB, using all four metrics improved the accuracy of the AGB estimation (see Supplement). Testing for the relative importance of each height metric, we found that all four metrics explained about 80 % of the variation in forest biomass at 1-ha scale,

and relatively less variations at 0.25 ha (58 %) and 0.04 ha (32 %). The relative contribution of the height metrics at 1-ha were 16 %, 19 %, 30 %, and 15 % respectively for RH25, RH50, RH75, and RH100. The influence of spatial scale on AGB is examined here by again comparing the results obtained using 0.04 ha, 0.025 ha and 1 ha subplots, using the cross-validated data. Figure 3 shows that for both LVIS and DRL data, the accuracy of AGB estimation increases when larger subplots are used. We found a strong relationship between ground AGB and Lidar estimated AGB when using 1 ha subplots in the model, with similar results for both LVIS and DRL data ($R^2_{LVIS} = 0.62$ and $R^2_{DRL} = 0.70$, $RMSE_{LVIS} = 31.7\,Mg\,ha^{-1}$ and $RMSE_{DRL} = 27.5\,Mg\,ha^{-1}$). At the 0.04 ha scale, the estimation accuracy was lower than at the 1 ha scale ($R^2_{LVIS} = 0.19$ and $R^2_{DRL} = 0.29$, $RMSE_{LVIS} = 187.5\,Mg\,ha^{-1}$ and $RMSE_{DRL} = 175.3\,Mg\,ha^{-1}$). Bias is very low when using 1 ha plots ($B_{LVIS} = -1.1\,Mg\,ha^{-1}$, $B_{DRL} = -0.2\,Mg\,ha^{-1}$), while bias reaches between $-23.9\,Mg\,ha^{-1}$ (for LVIS) and $-20.4\,Mg\,ha^{-1}$ (for DRL) when using 0.04 ha subplots. When not using cross-validation, $R^2_{LVIS} = 0.71$ and $R^2_{DRL} = 0.75$ at the 1 ha scale.

3.3 Lidar derived biomass change

Over the 50 ha plot, both ground and Lidar analyses indicate that on average, AGB decreased by $8\,Mg\,ha^{-1}$ between 2000 to 2010 ($AGB_{Change\_Ground} = 7.8\,Mg\,ha^{-1}$, $AGB_{Change\_Lidar} = -7.7\,Mg\,ha^{-1}$). At the 1 ha scale, the noise caused by estimation errors due to our regression model was large and only biomass changes greater than $22.6\,Mg\,ha^{-1}$ (standard deviation of Lidar-derived AGB change) could be detected unambiguously from Lidar data. Thirty-four of the fifty subplots showed the same direction (biomass gain or loss between the two dates) comparing the ground and Lidar-estimated AGB change (Fig. 4), with no regard of the $22.6\,Mg\,ha^{-1}$ threshold. For eleven of the remaining sixteen plots, AGB change between 2000 and 2010 is smaller than $22.6\,Mg\,ha^{-1}$ and therefore within the uncertainty threshold, in both ground and Lidar estimations. The remaining five 1 ha plots showed significantly opposite directions

in Lidar and ground estimations. The difference between ground and Lidar estimation of AGB change was much larger with smaller subplots (Fig. 5). For example, 3 ha of the 50 ha plot have been classified as secondary forest (dominated by the tree species *Gustavia superba*). The ground data analysis indicates that AGB increased in these secondary plots between 2000 and 2010 (mean AGB change$_{(secondary)}$ varies between +0.9 (0.04 ha scale) and +4.0 Mg ha^{-1} (1 ha scale)). However, Lidar only had a positive AGB change for this area at a large scale (mean AGB change$_{(secondary)}$ = +12.3 Mg ha^{-1} at 1 ha scale) and did not show the same trend at finer spatial scales, with a mean AGB change$_{(secondary)}$ of −13.1 Mg ha^{-1} at 0.04 ha and −6.7 Mg ha^{-1} at 0.25 ha. Hence even with small footprint Lidar, it is unlikely that quantitative changes in AGB will be accurately quantified at scales lower than 1 ha.

The ground and Lidar detection of changes had better agreements when the scale of analysis increased. At a 10 ha scale, the estimation of change could be predicted at about 6 Mg ha^{-1} over 10 yr, or less than 1 Mg ha^{-1} yr^{-1}. Table 4 shows how spatial scale affects Lidar-derived AGB change estimations at the plot level. Both Lidar-derived AGB change and the difference between Lidar and Field estimates decrease as the scale becomes coarser. The amplitude of differences between field-estimated change and Lidar-estimated change decreases quickly with increasing the scale of analysis, going from ±6.3 Mg ha^{-1} yr^{-1} at 1 ha to ±1.1 Mg ha^{-1} yr^{-1} at 25 ha. These results show that large spatial scales such as 10 ha or 25 ha give accurate AGB change estimations when looking at the 50 ha plot, but the 1 ha scale still seems to be a good option when looking for spatial patterns.

3.4 Whole-island estimates

Estimated AGB stocks and changes were then mapped across the entire island (1500 ha) using the equations developed at the plot level at 1 ha resolution, for both LVIS and DRL data. These two maps were then used to create an AGB change map (Fig. 6). A mask consisting of a one pixel erosion was applied to the final map to avoid

errors induced by edge effects. Hence, all the pixels that were on the edges of the island and contained errors were removed. The AGB change map shows that 32 % of the island had gained biomass between 2000 and 2010, while 35 % lost biomass. The remaining 33 % did not show significant trends during the period (changes less than ±10.5 Mg ha^{-1}). Mean AGB change over the whole island was found to be −3.6 Mg ha^{-1} (std = 37.2 Mg ha^{-1}), or −0.4 Mg ha^{-1} yr^{-1}. Patterns related to the forest age (Fig. 7b) and stage of regeneration can be seen in the AGB change map. Combining the AGB change map and the age map shows that old growth forest areas lost a lot of AGB (change = −7.2 ± 34.9 Mg ha^{-1}) whereas secondary forests gained AGB (change = +3.9 ± 33.8 Mg ha^{-1}) between 2000 and 2010. Standard deviation remained high for both forest age classes.

4 Discussion

The goal of our research was to study the ability of Lidar technology to estimate and map AGB changes when calibrated and combined with the field data. The relationship between Lidar-derived vertical canopy distribution and ground-based estimated AGB at plot level was used to create predictive equations for AGB at a landscape scale. A large number of studies have recently focused on AGB estimations in tropical forest using Lidar technology (Drake et al., 2002; Asner et al., 2011; Mascaro et al., 2011b) but to our knowledge, only one has been able to detect AGB changes from repeated Lidar measurements (Dubayah et al., 2010). Moreover, Dubayah et al. (2010) used the same sensor to detect AGB changes, whereas this study is the first to use two different sensors. Here we review our findings and discuss them in light of this recent literature and address the following questions associated with the biomass changes in old growth tropical forests: (1) can changes in biomass create a distinct and directional changes in vertical profile of the forest over time? (2) To what extent can these changes be detected by repeated measurements of the Lidar profiles?

The loss of approximately 0.8 $Mg\,ha^{-1}\,yr^{-1}$ of forest biomass derived from both ground and Lidar data over the 50 ha BCI plot may not be surprising, but it runs against recently published results over both Amazonian (Baker et al., 2004) or African (Lewis et al., 2010) forests. The loss of biomass in the old growth forest in BCI has been attributed to short-term disturbance such as the droughts from El Nino and subsequent changes in forest composition (Chave et al., 2008; Feeley et al., 2011). The role of lianas, which have been shown to increase in dominance in this forest (Wright et al., 2004) may also help explain this trend as the liana distribution has been shown to be associated with stands with low stature and canopy heights (Dalling et al., 2012). Also, as lianas become more dominant (Phillips et al., 2000) they tend to impose a higher load on large trees, resulting in increasing the risk of the tree falling (Chao et al., 2010).

Droughts have been considered as the main culprit for the biomass loss in tropical forests (Nepsted et al., 2005; Phillips et al., 2009; Lewis et al., 2011). In most studies, it was hypothesized that the biomass from a severe drought event can be followed with recovery and biomass gain immediately or after few years (Phillips et al., 2009). However, here we show that the impact of the drought may be longer that few years (about 10 yr).

A detailed analysis of the field inventory data suggest that the largest decline in biomass has been in DBH classes larger than 40 cm with the most significant loss (46.2 $Mg\,ha^{-1}$) in trees greater than 70 cm in diameter that include primarily the canopy or emergent trees (Fig. 7).

4.1 Use of Lidar height metrics

Differences in one height metric derived from Lidar waveforms (e.g. RH50, RH00, or Mean Canopy Height (MCH)) had no significant relationship with differences in forest biomass derived from the analysis of field surveys. This result suggested that we could not map the changes of forest biomass by directly analyzing the Lidar heights at 1-ha scale using two different sensors. Using the same sensor for both dates can

potentially provide a more reliable and height difference to calculate AGB change directly from Lidar (Dubayah et al., 2010). The indirect estimate of biomass change from Lidar data, however provided similar results as the field observations at the landscape scales (> 10 ha). By segmenting the Lidar derived biomass changes in the 50-ha plot into different biomass classes, the predicted changes point to regions of old growth with taller canopy trees (> 40 cm) as the main contributor of the overall decline in forest biomass in the 50 ha plot (Fig. 8).

We tested the performance of the models against other common equations used in the literature and concluded that for our datasets, use of several height metrics always outperformed the use of a single height metric such as mean canopy height or height of the median energy (Asner et al., 2009; Mascaro et al., 2011; Drake et al., 2002). Although different height metrics are correlated, each may provide a slightly different slice of vertical structure of the forest canopy and together they improve detection of variation in basal area, tree density, and the structural representation of wood density (trees in different diameter classes or successional states). Indeed, each metric should give specific structural information about the forest. For example, RH25 may improve quantification of changes in biomass from regeneration of understory trees and young saplings. A low RH25 may indicate that there is a lot of understory vegetation in the forest; whereas a RH25 close to RH50 may indicate that the understory contains few individuals, and that the plot is mainly composed of tall trees. The dynamics of these combined height metrics, if accurately quantified, hence may provide a more accurate picture of how forests are growing than can be obtained with a single metric. More work studying the relationship between RH metrics and size classes of trees can test these relationships.

4.2 Spatial scale of forest dynamics

The linear relationship between Lidar metrics and biomass estimates was found to be stronger as the pixel scale became coarser. High coefficients of correlation (R^2_{LVIS} = 0.62 and R^2_{DRL} = 0.70), low RMSE ($RMSE_{mean}$ = 29.6 $Mg\,ha^{-1}$) indicate that

the 1 ha scale is the best spatial scale to use in this type of analysis, as it gives more accurate results and minimizes the errors related to both field data and remote sensing data. At a 0.04 ha scale, we found a poor correlation (r^2_{LVIS} = 0.19 and r^2_{DRL} = 0.29) between ground-estimated AGB and Lidar-estimated AGB because the relationship is affected by high AGB variation due to events such as tree falls, compositional variations and gap regeneration, not necessarily detected to the same accuracy in the field data and the Lidar data. Although one could argue that a 0.04 ha spatial scale would be useful in studies related to gap analysis, such a small scale is not necessary for our study and AGB change analyses.

Tree geolocation errors on the ground and tree crown position relative to trunk position are other sources of error. These issues are magnified as the subplot size decreases. The aggregate effects of these small-scale changes at larger plots or stand level define the forest carbon dynamics at annual or multi-year temporal scales.

An encouraging result of this study is that the level of accuracy for AGB estimates from DRL and LVIS are similar, despite the differences in sensor design, spatial resolution and footprint size. It opens possibilities in terms of biomass change detection using Lidar data for future studies. Although it is always preferable to perform a change analysis using matching datasets at two different dates, our study shows that it is possible to perform this type of analysis using different sensors without affecting the quality of the results.

Although field and Lidar AGB change estimates are similar over the 50 ha plot (mean change = $-7.8\,Mg\,ha^{-1}$ between 2000 and 2010), the noise at 1 ha scale is too large to assess biomass change accurately and quantitatively at the plot level. Small changes in biomass are difficult to model at this scale. As a result, average changes at the plot level may be difficult to establish accurately, unless the changes are large. Still, we were able to estimate the change qualitatively and predict the sign of the biomass change (biomass gain or biomass loss) in 68 % of the 1-ha subplots.

In a recent study, Mascaro et al. (2011b) analyzed error predictions in terms of AGB and carbon stocks on BCI through two analyses using airborne Lidar data and ground

inventory data. They first tested the prediction of Asner et al. (2010) that spatial errors would scale with the inverse of the square root of pixel area as spatial resolution changes. They then analyzed the importance of plot-edge discrimination errors in AGB estimations. At 1 ha scale, they found an RMSE of $11.1\,Mg_{Carbon}\,ha^{-1}$, which corresponds to an RMSE of $22.2\,Mg\,ha^{-1}$ in terms of AGB, when not using their stem-localized approach. This result is similar to ours, since we found a mean RMSE of $29.6\,Mg\,ha^{-1}$ at the same scale. They further suggest that this RMSE could be reduced by accounting for canopy shape, which is essentially accounting for border effects in small subplots. Although this is a sensible approach, we refrained from implementing it because crown shape and size is seldom available in ground datasets, and we feel that the uncorrected RMSE reflects more accurately the inherent ability of the Lidar technology to infer tropical forest AGB. Further, at the 1 ha scale, this correction results only in a marginal reduction of the error (Mascaro et al., 2011a, Fig. S1), with $RMSE_{corrected} = 10.7\,Mg_{Carbon}\,ha^{-1}$ against $RMSE_{uncorrected} = 11.1\,Mg_{Carbon}\,ha^{-1}$.

Another difference of our study with that of Mascaro et al. (2011a) is that they used a calibration model between a single Lidar metric (MCH) and AGB, including early successional forest plots far away from BCI. Although this would be helpful to map AGB of the whole canal zone, it results in artificially inflating the R^2 of the model when just mapping BCI. Instead we used four Lidar-derived height metrics to estimate AGB directly from the 50-ha plot data, providing a more realistic error estimates for mapping the old growth forest biomass. Our approach also helps counter-balance the effects caused by the limited AGB range in the plot. Because the permanent plot is located in an old growth forest, there was no low biomass subplot. Using the four relative height metrics takes as much forest variation into account as possible. Thus, although the RH metrics are strongly correlated, we show in our analysis that using the four of them gives better results (see Supplement).

4.3 Variation of forest dynamics across the island

Landscape-level AGB changes at 1 ha resolution of the old-growth and younger forest match changes expected from forest succession theory (Shugart, 1984). Mean AGB change over the whole island is $-3.6\,\mathrm{Mg\,ha^{-1}}$ between 2000 and 2010, with most of the old growth forest being neutral or losing AGB (average change = $-7.2\,\mathrm{Mg\,ha^{-1}}$) while secondary forests gained AGB (average change = $+3.9\,\mathrm{Mg\,ha^{-1}}$). Previous ground-based studies over the BCI plot already reported this trend for the 2000–2005 interval (Chave et al., 2008). The fact that 100-yr old secondary forests still are aggrading carbon also is an important finding of this study.

Mascaro et al. (2011a) recently published an AGB map of BCI based on a similar approach. They found that AGB was lower in young forests than in mature forests. Here, we provide the first map of AGB changes and we show that young forests are increasing in AGB as expected.

Dubayah et al. (2010) performed the first AGB change study in a tropical forest. Their study was conducted at La Selva research station, Costa Rica. Their study presents some major differences with our study in terms of methodology. Dubayah et al. (2010) compared two LVIS datasets for the change analysis, while we are comparing one small footprint DRL and one LVIS dataset. In their study, Dubayah et al. (2010) performed a footprint-to-footprint comparison of the data and of height metrics. Their approach made it simpler to conduct an AGB change analysis by directly using change in Lidar-derived height between two dates, and change in ground estimated AGB between two dates. Our approach was less direct, but we avoided the issue of DEM location in LVIS. In doing so, we set the stage for many forthcoming Lidar studies based on a range of operating instruments. Despite these differences, the results of Dubayah et al. (2010) and ours are comparable in terms of AGB change trends. Indeed, Dubayah et al. (2010) showed that old growth forest was mostly neutral (average AGB change between 1998 and 2005 is $1.9\,\mathrm{Mg\,ha^{-1}}$), while secondary forests are gaining biomass (average change between 1998 and 2005 is $25.2\,\mathrm{Mg\,ha^{-1}}$).

4.4 Sources of errors

This study assumes Lidar height metrics can be used to detect biomass changes in old-growth and undisturbed tropical forest. An underlying hypothesis is that changes in biomass in the forest are related to changes in forest height or vertical structure. Unfortunately, this hypothesis is difficult to test based on literature data. Long-term studies in BCI and other sites have revealed that changes in forest structure and dynamics have complex trajectories and are often driven by many factors including random population fluctuations, climate disturbance, large scale successional or gap phase processes, and increasing resource availability or carbon fertilization (Feeley et al., 2011; Chave et al., 2008; Baker et al., 2004; Lewis et al., 2004, 2010; Clark et al., 2003, 2010). Over the past 25 yr the BCI plot has seen a high turnover, with almost 50 % of the initial individuals dying and being replaced. However, BCI forest structure studies include trees > 1 cm DBH while most similar studies only include trees > 10 cm DBH. This difference could explain BCI's apparently high turnover.

Some limitations related to both field data and Lidar data need to be discussed to better understand our results and the errors that we reported. First, the time difference between the field inventory and the acquisitions of Lidar data is a source of error that is hard to quantify in our analysis. Events such as tree falls might have happened between 1998 (LVIS data acquirement) and 2000 and between 2009 (DRL data acquirement) and 2010, causing error in model calibration, particularly at smaller scales, where the whole subplot would be affected.

The error associated with field data is also difficult to quantify. Although outliers in trunk diameter measurement are corrected before they are used in allometric equations, other errors related to fieldwork, such as tree geolocation errors, cannot be backtracked. Tree location errors can cause ambiguity in relating Lidar metrics to forest structure and biomass around the edges of plots and may introduce error in estimating the forest biomass and uncertainty in detecting small changes of biomass. This effect is minimized in the BCI dataset because of the intensive effort paid in the field.

Yet, it may be one of the causes of errors in estimating the biomass change at 1 ha scale over 10 yr period if this method is to be extended to more sites. Moreover, errors can occur even when the trunk geolocation is accurate. Trees can bend or have odd-shaped crowns, which will show in the Lidar data but will be impossible to detect using ground data. By increasing the plot size to 10 ha, the relative contribution of this error decreases, allowing the Lidar data to detect changes accurately.

Our study is also limited by the fact that our calibration excluded young secondary forest plots. Our allometric equation and our regression models were created using the 50 ha plot data, located in a mostly old secondary and old growth forest. The model was then applied to the entire island, composed of both old growth and secondary forests, especially on the eastern part of the island. As a result, our model should better predict old growth forest areas than secondary forest areas.

Although we obtained good results for both LVIS and DRL-derived biomass estimates, the fact that they are different sensors and have different characteristics (different footprint and RH metrics) limits our ability to understand the errors related to our study. Indeed, it is hard to know to what extent our change analysis error is due to the sensors or to other sources of error.

5 Conclusions

This study shows that Lidar can be used to analyze tropical forest dynamics on a decadal scale. Unlike other remote sensing technologies, Lidar is able to provide information on vertical forest structure, which makes it a unique tool to study and understand AGB and its dynamics through time at the landscape scale. Although AGB changes are hard to quantify at the plot level using Lidar data only, scaling up these changes at a landscape scale is a fundamental objective to understand the dynamics of forest succession. We demonstrated that there is no advantage in using spatial scales that belong to the same range as tree crown sizes when estimating AGB

change, especially at a landscape scale. Larger spatial scales, such as 1 ha, give more accurate results and should be preferred to finer scales in future studies.

Supplementary material related to this article is available online at: http://www.biogeosciences-discuss.net/10/1957/2013/bgd-10-1957-2013-supplement.pdf.

Acknowledgements. We thank Richard Condit for providing the field data (2010). We would also like to thank the many workers who collected the field data and made possible the assembly of the BCI census. The DRL dataset were obtained with funding from NSF grant 0939907, and with additional support from the Smithsonian Tropical Research Institute, University of Illinois, University of California Los Angeles, and Clemson University to SJ DeWalt. This work has benefited from French "Investissement ddvestis" grants (CEBA: ANR-10-LABX-0025; TULIP: ANR-10-LABX-0041) and from TOSCA funds (CNES, France).

References

Asner, G., Mascaro, J., Muller-Landau, H., Vieilledent, G., Vaudry, R., Rasamoelina, M., Baker, T. R., Phillips, O. L., Malhi, Y., Almeida, S., Arroyo, L., Di Fiore, A., Erwin, T., Higuchi, N., Killeen, T. J., Laurance, S. G., Laurance, W. F., Lewis, S. L., Monteagudo, A., Neill, D. A., Nunez Vargas, P., Pitman, N. C. A., Silva, J. N. M., Vasquez Martinez, R.: Increasing biomass in Amazonian forest plots, Philos. T. Roy. Soc. Lond. B, 359, 353–365, 2004.

Asner, G. P., Powell, G. V. N., Mascaro, J., Knapp, D. E., Clark, J. K., Jacobson, J., Kennedy-Bowdoin, T., Balaji, A., Paez-Acosta, G., Victoria, E., Secada, L., Valqui, M., and Hughes, R. F.: High- resolution forest carbon stocks and emissions in the Amazon, P. Natl. Acad. Sci. USA, 107, 16738–16742, 2010.

Baker, T. R., Phillips, O. L., Malhi, Y., Almeida, S., Arroyo, L., Di Fiore, A., Erwin, T., Higuchi, N., Killeen, T. J., Laurance, S. G., Laurance, W. F., Lewis, S. L., Monteagudo, A., Neill, D. A., Vargas, P. N., Pitman, N. C. A., Silva, J. N. M., and Martínez, R. V.: Increasing biomass in Amazonian forest plots, Philos. T. Roy. Soc. Lond. B, 359, 353–365, 2004.

Bohlman, S. and O'Brien, S.: Allometry, adult stature and regeneration requirement of 65 tree species on Barro Colorado Island, Panama, J. Trop. Ecol., 22, 123–136, 2006.
Chambers, J. Q., dos Santos, J., Ribeiro, R. J., and Higuchi, N.,: Tree damage, allometric relationships, and above-ground net primary production in central Amazon forest, Forest Ecol. Manag., 152, 73–84, 2001.
Chave, J., Condit, R., Aguilar, S., Hernandez, A., Lao, S., and Perez, R.: Error propagation and scaling for tropical forest biomass estimates, Philos. T. Roy. Soc. Lond. B, 359, 409–420, 2004.
Chave, J., Andalo, C., Brown, S., Cairns, M., Chambers, J., Eamus, D., Fölster, H., Fromard, F., Higuchi, N., Kira, T., Lescure, J. P., Nelson, B., Ogawa, H., Puig, H., Riéra, B., and Yamakura, T.: Tree allometry and improved estimation of carbon stocks and balance in tropical forests, Oecologia, 145, 87–99, 2005.
Chave, J., Condit, R., Muller-Landau, H. C., Thomas, S. C., Ashton, P. S., Bunyavejchewin, S., Co, L. L., Dattaraja, H. S., Davies, S. J., Esufali, S., Ewango, C. E. N., Feeley, K. J., Foster, R. B., Gunatilleke, N., Gunatilleke, S., Hall, P., Hart, T. B., Hernandez, C., Hubbell, S. P., Itoh, A., Kiratiprayoon, S., LaFrankie, J. V., de Lao, S. L., Makana, J. R., Noor, M. N. S., Kassim, A. R., Samper, C., Sukumar, R., Suresh, H. S., Tan, S., Thompson, J., Tongco, M. D. C., Valencia, R., Vallejo, M., Villa, G., Yamakura, T., Zimmerman, J. K., and Losos, E. C.: Assessing evidence for a pervasive alteration in tropical tree communities, Plos Biol., 6, 455–462, 2008.
Clark, D. A., Piper, S. C., Keeling, C. D., and Clark, D. B.: Tropical rain forest tree growth and atmospheric carbondynamics linked to interannual temperature variation during 1984–2000, P. Natl. Acad. Sci. USA, 100, 5852–5857, 2003.
Clark, D. B. and Clark, D. A.: Landscape-scale variation in forest structure and biomass in a tropical rain forest, Forest Ecol. Manag., 137, 185–198, 2000.
Clark, D. B., Clark, D. A., and Oberbauer, S. F.: Annual wood production in a tropical rain forest in NE Costa Rica linked to climatic variation but not to increasing CO_2, Glob. Change Biol., 16, 747–759, 2010.
Condit, R.: Research in large, long-term tropical forest plots, Trends Ecol. Evol., 10, 18–22, 1995.
Condit, R., Watts, K., Bohlman, S. A., Perez, R., Foster, R. B., and Hubbell, S. P.: Quantifying the deciduousness of tropical forest canopies under varying climates, J. Veg. Sci., 11, 649–658, 2000.

Croat, T. B.: Flora of Barro Colorado Island, Stanford University Press, Stanford, CA, 1978.
Dalling, J. W., Schnitzer, S. A., Baldeck, C., Harms, K. E., John, R., Mangan, S. A., Lobo, E., Yavitt, J. B., and Hubbell, S. P.: Resource-based habitat associations in a neotropical liana community, J. Ecol., 100, 1174–1182, 2012.
Drake, J. B., Dubayah, R. O., Clark, D. B., Knox, R. G., Blair, J. B., Hofton, M. A., Chazdon, R. L., Weishampel, J. F., and Prince, S.: Estimation of tropical forest structural characteristics using large-footprint lidar, Remote Sens. Environ., 79, 305–319, 2002a.
Drake, J. B., Dubayah, R. O., Knox, R. G., Clark, D. B., and Blair, J. B.: Sensitivity of large-footprint lidar to canopy structure and biomass in a neotropical rainforest, Remote Sens. Environ., 81, 378–392, 2002b.
Drake, J. B., Knox, R. G., Dubayah, R. O., Clark, D. B., Condit, R., Blair, J. B., and Hofton, M.: Above-ground biomass estimation in closed canopy Neotropical forests using lidar remote sensing: factors affecting the generality of relationships, Global Ecol. Biogeogr., 12, 147–159, 2003.
Dubayah, R. O., Sheldon, S. L., Clark, D. B., Hofton, M. A., Blair, J. B., Hurtt, G. C., and Chazdon, R. L.: Estimation of tropical forest height and biomass dynamics using lidar remote sensing at La Selva, Costa Rica, J. Geophys. Res., 115, G00E09, doi:10.1029/2009JG000933 2010.
Duong, V. H., Lindenbergh, R., Pfeifer, N., and Vosselman, G.: Single and two epoch analysis of ICESat full waveform data over forested areas, Int. J. Remote Sens., 29, 1453–1473, 2008.
Enders, R. K.: Mammalian life histories from Barro Colorado Island, Panama, Bull. Mus. Comp. Zool., 78, 385–502, 1935.
Feeley, K. J., Davies, S. J., Perez, P., Hubbell, S., and Foster R: Directional changes in the species composition of a tropical forest, Ecology, 92, 871–882, 2011.
Foster Jr., R. B.: Structure and history of the vegetation of Barro Colorado Island, in: The Ecology of a Tropical Forest Seasonal Rhythms and Long-Term Changes, edited by: Brokaw, N., Smithsonian Institution Press, Washington DC, 67–82, 1982.
Fricker, G. A., Saatchi, S. S., Meyer, V., Gillespie, T. W., and Sheng, Y.: Application of semi-automated filter to improve waveform Lidar sub-canopy elevation model, Remote Sens., 4, 1494–1518, 2012.
Kellner, J. R. and Asner, G. P.: Convergent structural responses of tropical forests to diverse disturbance regimes, Ecol. Lett., 12, 887–897, 2009.

Kenoyer, L. A.: General and successional ecology of the lower tropical rain-forest at Barro Colorado Island, Panama, Ecology, 10, 201–222, 1929.
Lefsky, M. A., Cohen, W. B., Parker, G. G., and Harding, D. J.: Lidar remote sensing for ecosystem studies, BioScience, 52, 19–30, 2002.
Leigh, E. G.: Tropical Forest Ecology: A View from Barro Colorado Island, Oxford University Press, New York Oxford, 1999.
Leigh, E. G. and Wright, S. J.: Barro Colorado Island and tropical biology, in: Four Neotropical Rainforests, edited by: Gentry, A. H., Yale University Press, New Haven, USA, 28–47, 1990.
Leigh, E. G., Loo de Lao, S., Condit, R. G., Hubbell, S. P., Foster, R. B., and Perez, R.: Barro Colorado Island forest dynamics plot, Panama, in: Tropical Forest Diversity and Dynamism: Findings from a Large-Scale Plot Network, edited by: Losos, E. C. and Leigh, J., Egbert Giles, University of Chicago Press, Chicago, 451–463, 2004.
Lewis, S. L., Malhi, Y., and Phillips, O. L.: Fingerprinting the impacts of global change on tropical forests, Philos. T. Roy. Soc. B, 359, 437–462, 2004.
Lewis, S. L., Lopez-Gonzalez, G., Sonke, B., Affum-Baffoe, K., Baker, T. R., Ojo, L. O., Phillips, O. L., Reitsma, J. M., White, L., Comiskey, J. A., Djuikouo, M. N., Ewango, C. E. N., Feldpausch, T. R., Hamilton, A. C., Gloor, M., Hart, T., Hladik, A., Lloyd, J., Lovett, J. C., Makana, J.-R., Malhi, Y., Mbago, F. M., Ndangalasi, H. J., Peacock, J., Peh, K. S. H., Sheil, D., Sunderland, T., Swaine, M. D., Taplin, J., Taylor, D., Thomas, S. C., Votere, R., and Woll, H.: Increasing carbon storage in intact African tropical forests, Nature, 457, 1003–1006, 2009.
MacArthur, R. H. and Horn, H. S.: Foliage profile by vertical measurements, Ecology, 50, 802–804, 1969.
Mascaro, J., Asner, G. P., Muller-Landau, H. C., van Breugel, M., Hall, J., and Dahlin, K.: Controls over aboveground forest carbon density on Barro Colorado Island, Panama, Biogeosciences, 8, 1615–1629, doi:10.5194/bg-8-1615-2011, 2011a.
Mascaro, J., Detto, M., Asner, G. P., and Muller-Landau, H. C.: Evaluating uncertainty in mapping forest carbon with airborne Lidar, Remote Sens. Environ., 115, 3770–3774, 2011b.
McCullough, D.: The Path Between the Seas, Simon and Schuster, New York, NY, USA, 1977.
Ni-Meister, W., Jupp, D. L. B., and Dubayah, R.: Modeling Lidar waveforms in heterogeneous and discrete canopies, IEEE Trans. Geosci. Remote, 39, 1943–1958, 2001.
Saatchi, S. S., Harris, N. L., Brown, S., Lefsky, M., Mitchard, E. T. A., Salas, W., Zutta, B. R., Buermann, W., Lewis, S. L., Hagen, S., Petrova, S., White, L., Silman, M., and Morel, A.:

Benchmark map of forest carbon stocks in tropical regions across three continents. P. Natl. Acad. Sci. USA, 108, 9899–9904, 2011.
Shugart, H. H.: A Theory of Forest Dynamics, Springer, New York, NY, 1984.
Wright, S. J., Calderón, O., Hernandéz, A., and Paton, S.: Are lianas increasing in importance in tropical forests? A 17-year record from Panama, Ecology, 85, 484–489, 2004.

Table 1. Coefficients of the Lidar derived AGB equations.

$AGB_{LVIS} = (a_0 + a_1 RH25 + a_2 RH50 + a_3 RH75 + a_4 RH100 + a_5 RH100_{max})^2$

$AGB_{DRL} = (a_0 + a_1 RH25 + a_2 RH50 + a_3 RH75 + a_4 RH100)^2$

	a_0	a_1	a_2	a_3	a_4	a_5
LVIS 100 m	−0.887093	0.0331947	0.0904487	0.0358468	0.280236	0.0843859
DRL 100 m	0.78671	0.28463	−0.421906	0.519381	0.0850332	–

Table 2. 2010 AGB statistics, from field estimations. AGB is highly variable and its distribution is skewed toward low values when using 0.04 ha subplots, but becomes more stable at 0.25 ha and 1 ha.

AGB 2010 ($Mg\,ha^{-1}$)	0.04 ha	0.25 ha	1 ha
Mean	235.65	235.65	235.65
Std deviation	204.77	83.04	49.61
Skewness	3.05	0.78	0.45
Kurtosis	13.65	0.46	0.52
Min	21.6	88.60	116.14
Max	1838.92	567.21	369.13
Coef. of variation	0.87	0.35	0.21

Table 3. AGB Change (in Mg ha^{-1}) between 2000, 2005 and 2010, from field estimations, at three spatial scales. AGB decreased both between 2000 and 2005 and between 2005 and 2010 census periods in the 50 ha plot. AGB changes are more stable at 1 ha than at 0.04 ha.

	0.04 ha			0.25 ha			1 ha		
Time period	00/05	05/10	00/10	00/05	05/10	00/10	00/05	05/10	00/10
Mean change	−2.4	−5.5	−7.8	−2.4	−5.5	−7.8	−2.4	−5.5	−7.8
Std Dev.	58.6	93.6	107.4	24.7	37.7	41.7	10.6	16.1	17.6
Min Change	−701.7	−1749.3	−1522.7	−145.8	−288.9	−252.0	−44.4	−49.6	−47.0
Max change	237.9	1167.9	1196.4	37.0	177.9	172.1	11.2	45.7	40.3

Table 4. Lidar detected AGB change (in Mg ha^{-1} yr^{-1}) and difference between Lidar and field AGB change estimates in the 50 ha plot, at large spatial scales. Both AGB change and the difference between Lidar and field estimates decrease as the scale becomes coarser.

	Lidar detected AGB Change (mean = −0.77)		Difference between Lidar detected AGB Change and Field estimations (mean = 0.02)	
	Min	Max	Min	Max
1 ha	−6.28	4.30	−6.16	5.75
5 ha	−1.77	1.31	−1.36	1.73
10 ha	−1.34	0.75	−0.65	1.03
25 ha	−1.12	−0.41	−0.32	0.36

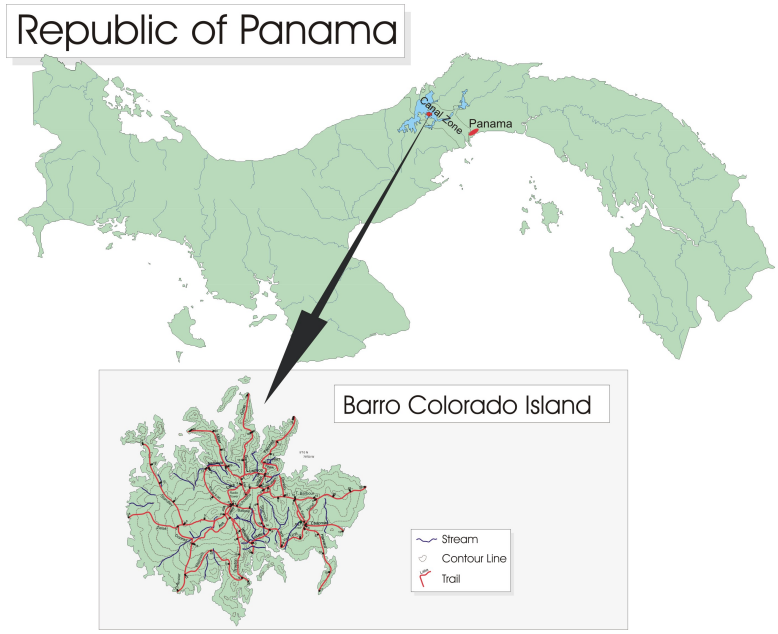

Fig. 1. Panama and Barro Colorado Island Map (Smithsonian Tropical Research Institute website).

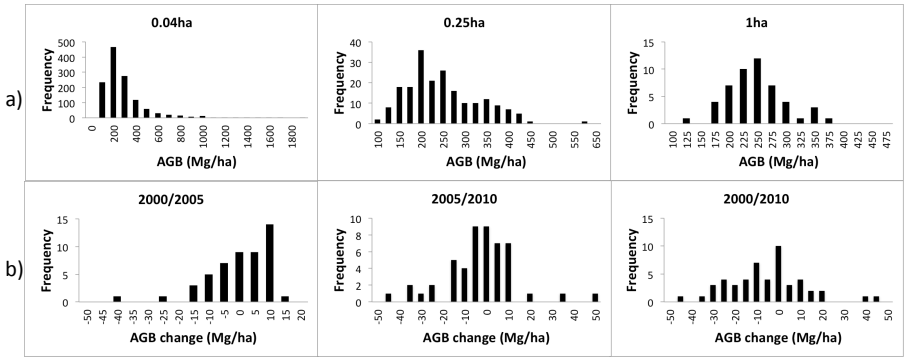

Fig. 2. (a) Histograms of AGB distribution in the permanent plot at three spatial scales. AGB distribution is skewed to the left when using 0.04 ha subplots. AGB distribution becomes normal when working with larger subplots, especially at 1 ha. **(b)** Histograms of AGB Change between 2000, 2005 and 2010 in the 50 ha plot (1 ha scale) . There are more extreme values (positive and negative) between 2005 and 2010, than between 2000 and 2005.

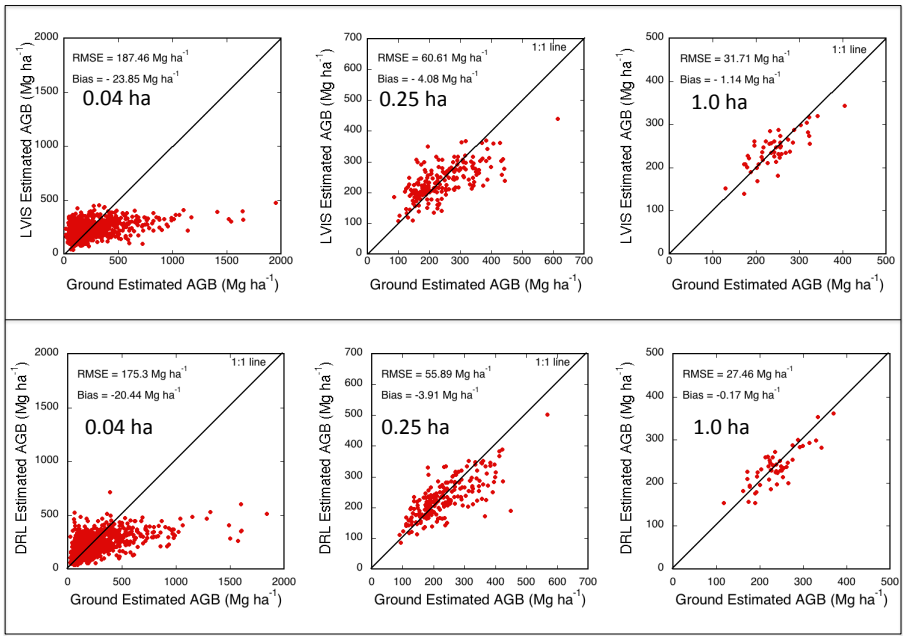

Fig. 3. Relationship between ground estimated AGB and Lidar (LVIS at the top and DRL at the bottom) estimated AGB. The correlation between the two metrics increases as the scale becomes coarser.

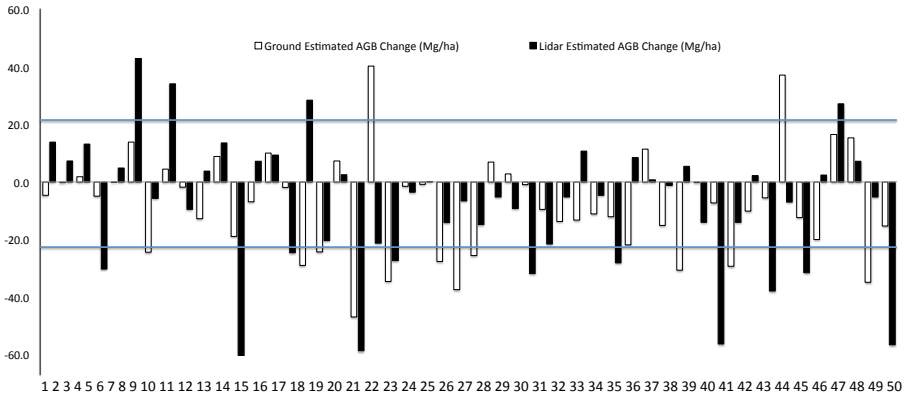

Fig. 4. Comparison of AGB change (Ground estimation vs. Lidar estimation) for every 1 ha subplot. The sign of AGB change was correctly predicted for thirty-four of the fifty subplots. Eleven of the sixteen subplots that do not match have AGB change values that are smaller than the Lidar-derived AGB change standard deviation (22.6 Mg ha^{-1}).

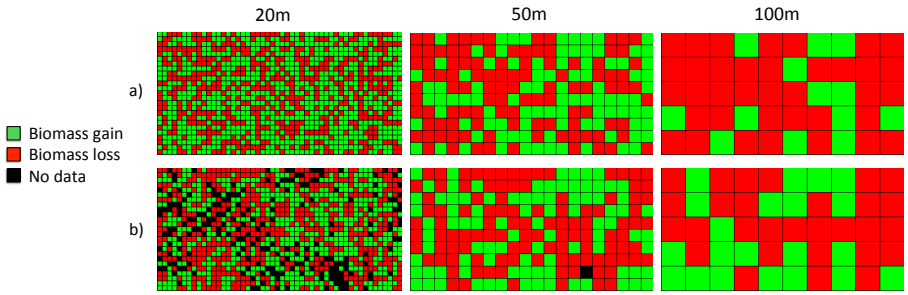

Fig. 5. AGB change (in $Mg\,ha^{-1}$) from Ground estimations **(a)** and from Lidar estimations **(b)** in the 50 ha plot, at 0.04 ha, 0.25 ha and 1 ha spatial scales. At these scales and at the plot level, Lidar estimates do not show the same AGB change trends as the ground estimates, although patterns can be seen at the 1 ha scale.

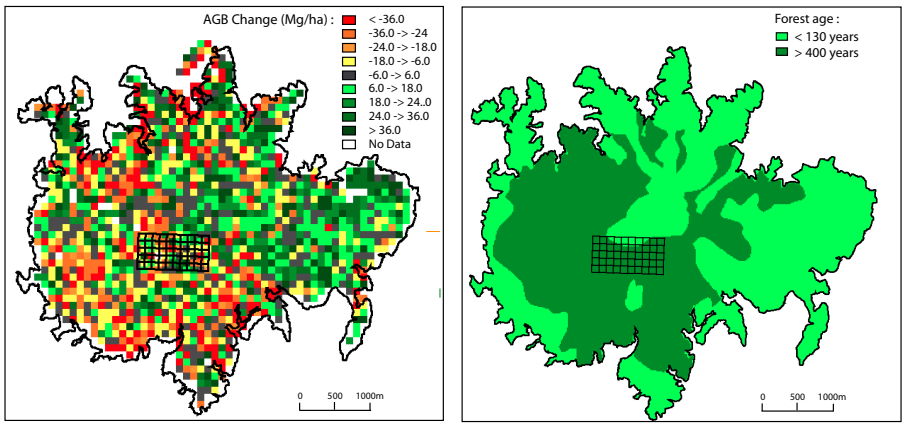

Fig. 6. AGB change map between 2000 and 2010 (left) and forest age map (right). AGB decreased in old growth forest (dark green in the age map), whereas the forest gained biomass in younger, regenerating forest (light green in the age map).

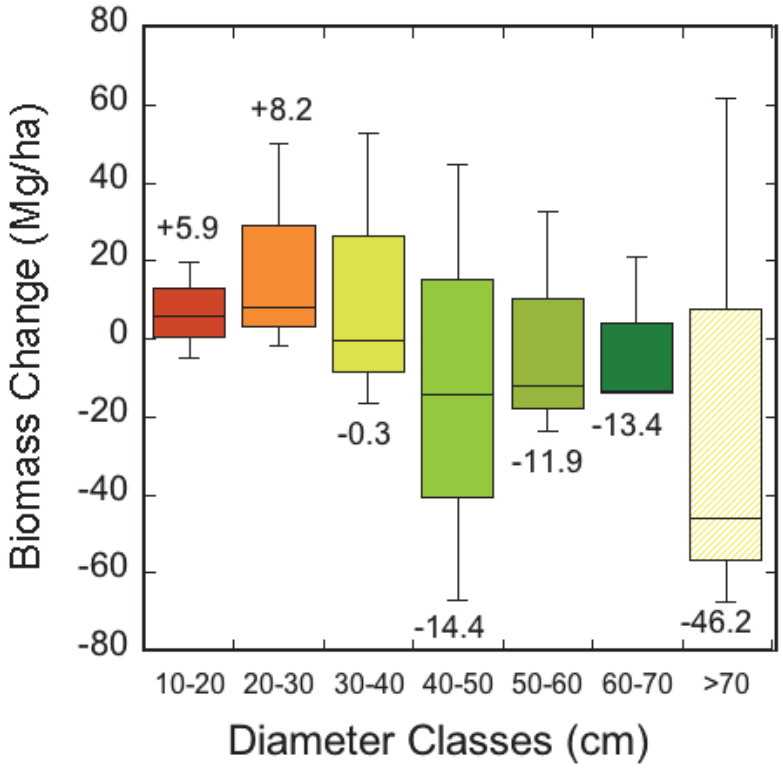

Fig. 7. DBH classes and AGB change (20 m spatial scale). AGB is increasing in small DBH classes while trees having DBH higher than 40 m are losing biomass.

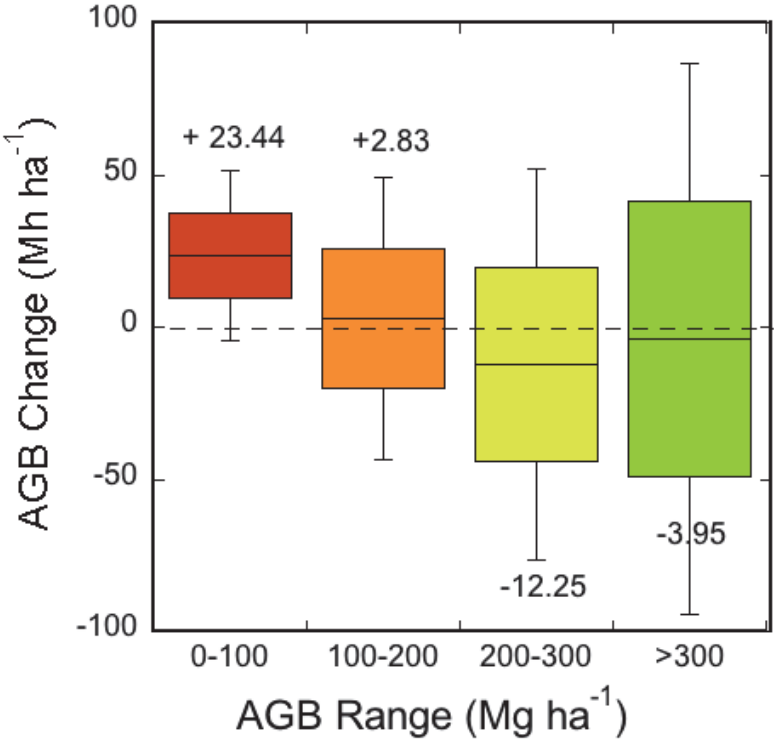

Fig. 8. Lidar-derived AGB range and AGB Change (20 m spatial scale). AGB in subplots with low biomass is increasing, while subplots with high biomass are losing biomass and contribute to the overall loss of biomass in BCI.